

## Dealuminated ZSM-5 Zeolite Catalyst for Ethylene Oligomerization to Liquid Fuels

Nor Aishah Saidina Amin<sup>1\*</sup>, Didi Dwi Anggoro<sup>1,2</sup>

1. Faculty of Chemical and Natural Resources Engineering, Universiti Teknologi Malaysia, 81310 Skudai, Johor, Malaysia

2. Department of Chemical Engineering, University of Diponegoro, Semarang 50232, Indonesia

[Manuscript received August 6, 2002; revised September 6, 2002]

**Abstract:** Ethylene oligomerization using ZSM-5 zeolite was investigated to study the role of Brönsted acid sites in the formation of higher hydrocarbons. The oligomerization of olefins, dependent on the acidity of ZSM-5 zeolite, is an important step in the conversion of natural gas to liquid fuels. The framework Si/Al ratio reflects the number of potential acid sites and the acid strength of the ZSM-5 catalyst. ZSM-5 with the mole ratio  $\text{SiO}_2/\text{Al}_2\text{O}_3$  equal to 30 was dealuminated for different periods of time according to the acidic ion-exchange method to produce ZSM-5 with various Si/Al ratios. The FT-IR analysis revealed that the integrated framework aluminum band, non-framework aluminum band, and silanol groups areas of the ZSM-5 zeolites decreased after being dealuminated. The performance of the dealuminated zeolite was tested for ethylene oligomerization. The results demonstrated that the dealumination of ZSM-5 led to higher ethylene conversion, but the gasoline selectivity was reduced compared to the performance of a ZSM-5 zeolite. The characterization results revealed the amount of aluminum in the zeolitic framework, the crystallinity of the ZSM-5 zeolite, and the Si/Al ratio affected the formation of Brönsted acid sites. The number of the Brönsted acid sites on the catalyst active sites is important in the olefin conversion to liquid hydrocarbons.

**Key words:** ethylene, liquid fuels, oligomerization, dealumination, ZSM-5

### 1. Introduction

The conversion of natural gas to liquid fuels can be carried out over bifunctional catalysts that are acidic and oxidative [1-3]. Normally, the dominant component of natural gas is methane ( $\text{CH}_4$ ). The mechanism of the reaction between methane and oxygen to produce liquid hydrocarbons over acidic zeolites is postulated to start from the formation of methyl radicals ( $\text{CH}_3^*$ ) from  $\text{CH}_4$  [4]. The methyl radicals combine to form ethane which dehydrogenates to ethylene. Ethylene will oligomerize further into higher hydrocarbons to form oxygenates, aromatics, and liquid fuels or be involved in deep oxidation to produce  $\text{CO}_2$  and  $\text{H}_2\text{O}$ .

The strength of oligomerization depends, among others factors, on the acidic sites of the zeolite [5-7]. For ethylene oligomerization over ZSM-5, both Brönsted and Lewis acid sites were observed to be active although Lewis sites have a small advantage in suppressing the coke formation [8]. The strong Brönsted acid sites eliminated coke or aromatic formation and allowed only oligomerization to proceed [8]. The amount of framework aluminum is related to the number of Brönsted acid sites [9].

The framework Si/Al ratio is a reflection of the number of potential acid sites [10]. For each particular zeolite structure the acidity per active site reached a maximum value at a particular Si/Al ratio, which determines the acidic strength of the zeo-

\* Corresponding author. Tel: 607-5505388; Fax: 607-5581463;  
E-mail address: r-naishah@utm.my.

lite [11,12]. High acid strength as well as high thermal and chemical stability are desirable properties that could be improved by increasing the framework Si/Al ratio. However, the vast majority of zeolites can only be synthesized with relatively low Si/Al ratios. Thus, the zeolites have to be subjected to various post-synthesis dealumination treatments to remove Al from the framework and increase the Si/Al ratio.

The purpose of this work is to investigate the relation of Brönsted acid sites formed by various dealumination durations with the ethylene oligomerization to liquid fuels. Ethylene is a very reactive component and by studying its oligomerization over ZSM-5 zeolite we hope to understand the relation of aluminum and the number of Brönsted acid sites to the oligomerization of olefins. The scope of this study is to dealuminate the ZSM-5 zeolite, characterize both the ZSM-5 and dealuminated ZSM-5 zeolites by FT-IR and XRD measurements, and examine the catalytic activity for ethylene conversion to liquid fuels.

## 2. Experimental

ZSM-5 zeolite (supplied by Zeolyst International in  $\text{NH}_4$  form; mole ratio  $\text{SiO}_2/\text{Al}_2\text{O}_3 = 30$ ; surface area =  $400 \text{ m}^2/\text{g}$ .) was dealuminated by treating it with 1 N HCl solution at  $80^\circ\text{C}$ . The dealumination treatment was carried out according to the method described elsewhere [11]. The samples were named DZ-1, DZ-2, and DZ-3 for 12, 24, and 36 hours of dealumination time, respectively.

XRD measurements were performed using a Philips 1840 with Cu  $K\alpha$  radiation,  $\lambda = 1.54056 \text{ \AA}$  at 40 kV and 30 mA in the range of  $2\theta = 2^\circ$  to  $60^\circ$ , a scanning speed of  $4^\circ$  per minute, and a vertical goniometer at room temperature. Samples were saturated over concentrated  $\text{NH}_4\text{Cl}$  solution in a desiccator to ensure complete dehydration before recording the pattern, as this can affect the lattice parameter. The powder was ground before it was mounted on a glass slide.

The mid-infrared spectra ( $1,500\text{--}400 \text{ cm}^{-1}$ ) were recorded on a Shimadzu FT-IR 8000 series using the KBr pellet technique. Infrared spectrums for the hydroxyl group were also recorded on a Shimadzu FT-IR 8000. An IR spectrum was acquired in the absorbance mode at  $25^\circ\text{C}$  in the wave number of  $4,000\text{--}1,300 \text{ cm}^{-1}$ , and with  $2 \text{ cm}^{-1}$  resolutions.

Thin wafers of 13 mm diameter were made by pressing about 10 mg of fine zeolite powder under five

tons of pressure for 15 seconds. The thin wafer was placed in a ring-type sample holder and transferred into the IR cell equipped with a  $\text{CaF}_2$  window. The IR cell containing the zeolite wafer was placed into the vacuum system ( $1 \times 10^{-8}$  mbar pressure). For hydroxyl group analysis, each zeolite sample was dehydrated at  $400^\circ\text{C}$  for five hours in a vacuum system. The infrared spectra of these samples were recorded at room temperature.

The performance of the catalysts was tested for ethylene conversion to liquid hydrocarbons (LHC) via a single step reaction in a fixed-bed micro-reactor over 1 gram of catalyst. Ethylene with 99.9% purity was reacted at atmospheric pressure and temperature of  $400^\circ\text{C}$  at ethylene flow rate of 50 ml/min and GHSV =  $3,000 \text{ ml}/(\text{g}\cdot\text{h})$ . The reactor was first preheated to  $400^\circ\text{C}$  under a 100 ml/min nitrogen stream for two hours to activate the catalyst. The reaction products were separated into liquid and gas components through an ice-trap. The gas and liquid products were analyzed by a gas chromatography using HP-1 capillary column equipped with an FID [13]. The catalysts were tested after five hours on stream and under that condition the catalysts were not severely deactivated.

## 3. Results and discussion

### 3.1. Characterization of zeolite

The FT-IR analysis of ZSM-5 and dealuminated ZSM-5 zeolite is shown in Figure 1. All catalyst samples illustrated bands at about  $546$  and  $1,223 \text{ cm}^{-1}$ . The results suggested that there is no change in the ZSM-5 crystalline structure after the dealumination treatment. From Figure 1, the spectra of ZSM-5 and dealuminated ZSM-5 did not exhibit a band at  $1,398 \text{ cm}^{-1}$ , which is typical of ammonium ions [14]. This result suggests that hydrogen ions had replaced the ammonium ions after calcination. A schematic diagram of the phenomena is depicted in Figure 2 [15].

There is a significant frequency shift or decrease in the intensity framework for the dealuminated samples (Figure 1) at  $1,099 \text{ cm}^{-1}$  frequency band, which can be attributed to the asymmetric stretching of framework Si–O–Si or Si–O–Al bonds [16]. The shift indicates that there is a significant change in the number of those forming, framework bonds [17]. Among the dealuminated samples, DZ-1 exhibits the lowest frequency band at  $1,099 \text{ cm}^{-1}$ . More aluminum atoms were probably removed from the DZ-1 zeolite framework than from the DZ-2 and DZ-3 samples. This

result is similar to the findings reported by Kooyman *et al.* [11]. Kumar *et al.* [12] reported that the SEM images illustrated no visible change in the particle and morphology after the dealumination of HZSM-5. However, the FT-IR spectra in Figure 1 revealed small amounts of extra framework Al due to OH stretching vibration at  $1,099\text{ cm}^{-1}$ .

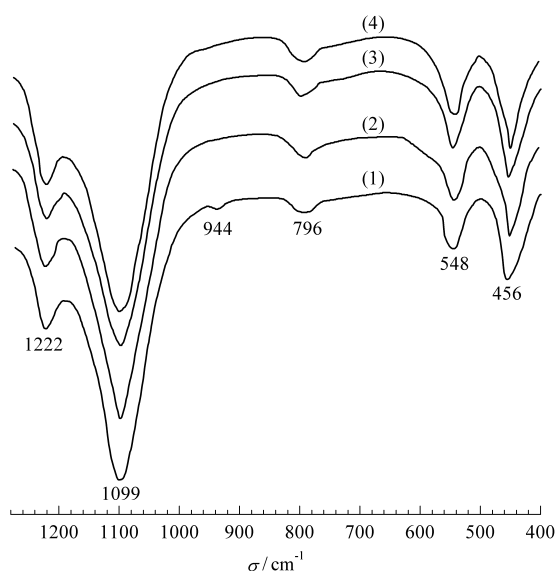


Figure 1. Mid-infrared spectra of (1) ZSM-5; (2) DZ-1; (3) DZ-2 and (4) DZ-3.

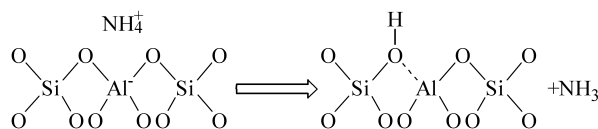


Figure 2. Schematic diagram of ammonium ions replaced by hydrogen ions [15].

The crystallinity of ZSM-5 can be determined by using the IR optical density ratio of the 546 and  $454\text{ cm}^{-1}$  bands of the zeolite [18]. The results in Table 1 show the optical density ratio of DZ-1 is the highest while ZSM-5 is the lowest. Nevertheless, the differences are small. Thus, it can be concluded from the optical density ratio that no significant change to the zeolite structure occurred upon dealumination.

Table 1. The optical density ratio of catalysts

Catalyst	$\sigma_{\text{band}_1}$	$\sigma_{\text{band}_2}$	Optical density ratio $\sigma_{\text{band}_1}/\sigma_{\text{band}_2}$
	( $\text{cm}^{-1}$ )	( $\text{cm}^{-1}$ )	
ZSM-5	447	547	0.817
DZ-1	462	547	0.845
DZ-2	454	547	0.829
DZ-3	452	546	0.828

The typical stretching vibrational band of the bridging OH groups bonded to tetrahedrally coordinated framework aluminum is located at  $\approx 3,610\text{ cm}^{-1}$ . For non-framework, or octahedral, Al sites, the band at  $3,660\text{ cm}^{-1}$  is assigned to the hydroxyl groups. The framework and non-framework hydroxyl groups are described in Figures 3 (a) and (b) [19].

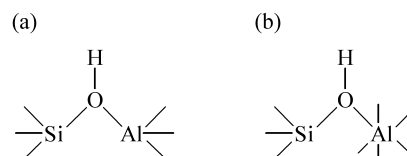


Figure 3. Structure of two types of terminal hydroxyl groups [19].

(a) Framework (tetrahedral), (b) Non-framework (octahedral).

Table 2 compares the OH region of the IR spectra of all the ZSM-5 zeolite samples with those of earlier investigators [20,21,12]. In the previous study, the vibration (OH) regions of the IR spectrum of a ZSM-5 zeolite contained bands at  $\approx 3,600$  and  $3,740\text{ cm}^{-1}$  while a band at  $\approx 3,649\text{ cm}^{-1}$  was ascribed to OH groups of the non-framework aluminum species. The band at  $\approx 3,736\text{ cm}^{-1}$  was assigned to terminal silanol groups attached to the framework [21]. The results in Table 2 indicate a similar occurrence of the OH region in previous and present studies.

Table 2. OH region of the IR Spectrum of ZSM-5 in the references and this study

Sample	$\sigma$ ( $\text{cm}^{-1}$ )		
	Framework-Al	Silanol	Non framework-Al
ZSM-5 [20]	3,610	3,745	3,665
ZSM-5 [21]	3,598	3,733	3,655
ZSM-5 [12]	3,610	3,735	3,665
ZSM-5	3,609	3,744	3,664
DZ-1	3,609	3,743	3,663
DZ-2	3,607	3,744	3,665
DZ-3	3,609	3,741	3,662

The vibration (OH) regions of the IR spectrum of ZSM-5 and dealuminated ZSM-5 zeolite catalysts are shown in Figure 4, where all the samples have bands at  $3,609\text{ cm}^{-1}$ ,  $3,664\text{ cm}^{-1}$ , and  $3,744\text{ cm}^{-1}$ . The spectra indicated that all the samples have aluminum framework, silanol, and aluminum non-framework groups. In addition, the spectra demonstrated that the appearance of this band at  $3,744\text{ cm}^{-1}$  is an indication of the crystallinity of the ZSM-5 zeolites being

reduced due to the increasing number of terminal Si-OH groups per unit cell [22].

The number of Brönsted acid sites ( $N_{\text{BAC}}$ ) can be calculated by bridging OH groups (at  $3,609 \text{ cm}^{-1}$  band) according to [23]:

$$N_{\text{BAC}} = (\text{Integrated area of } 3,609 \text{ cm}^{-1} \times 0.7857) / (4.05 \times 5.92), \mu\text{mole/g}$$

where, integrated Area ( $\text{cm}^{-1}$ ) of  $3,609 \text{ cm}^{-1}$  data is obtained from FT-IR equipment; the constant value of  $0.7857 \text{ cm}^2$  is surface area of sample (thin wafers); the constant value of  $4.05 \text{ cm} \cdot \mu\text{mole}^{-1}$  is from references [23]; the constant value of  $5.92 \text{ mg}$  is weight of sample.

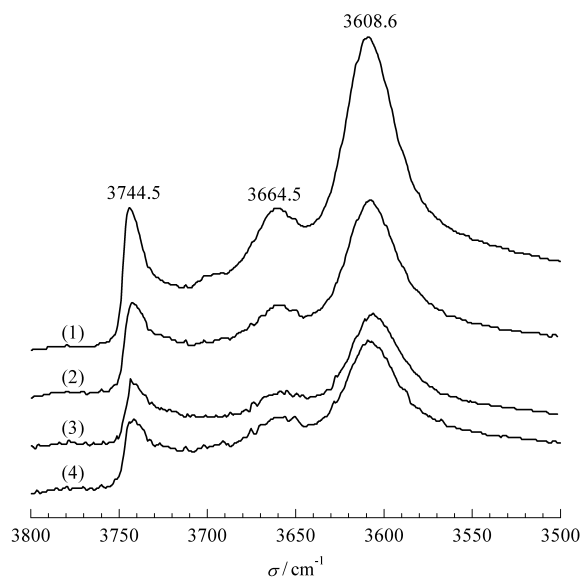


**Figure 4.** IR spectra in the hydroxyl stretch region of zeolite samples after dehydration at  $400 \text{ }^\circ\text{C}$  in  $1 \times 10^{-8} \text{ mbar}$  for 2 hours. (1) ZSM-5; (2) DZ-1; (3) DZ-2 and (4) DZ-3

Figure 5 demonstrates that the integrated band area of the framework aluminum ( $3,609 \text{ cm}^{-1}$ ) of all the dealuminated samples DZ-1, DZ-2, and DZ-3 (50.5, 40.5, and 14.6, respectively) are smaller than the ZSM-5 zeolite (91.2). The larger integrated band area of ZSM-5 indicates a large amount of framework aluminum in that sample. The amount of framework aluminum in the dealuminated samples decreased, possibly due to the extraction of aluminum from the zeolitic framework into the acidic solution. The  $N_{\text{BAC}}$  for the samples decreased in the following order: ZSM-5 > DZ-1 > DZ-2 > DZ-3.

The results in Figure 5 also indicate that the integrated band areas of the non-framework aluminum ( $3,664 \text{ cm}^{-1}$ ) for DZ-1, DZ-2, and DZ-3 (13.3, 7.9, and 5.4, respectively) are smaller than that of ZSM-

5 (26.9). The decrease in the integrated band areas of the dealuminated samples indicates that the amount of the non-framework aluminum decreased as well. This phenomenon is again attributed to the non-framework aluminum being extracted into the acidic solution.

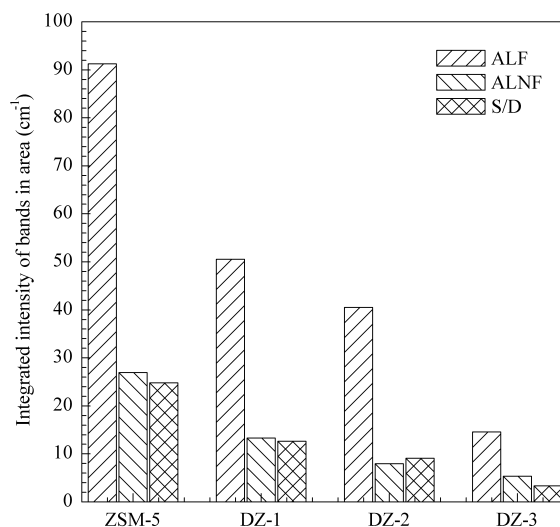


**Figure 5.** Integrated intensity of bands associated with bridging hydroxyls framework Al (ALF), extra-framework Al species (ALNF) and silanol group (S/D) in ZSM-5 and dealuminated ZSM-5.

The area of the silanol group is 12.7, 9.1, and 3.3 for DZ-1, DZ-2, and DZ-3, respectively (Figure 5). The silanol group area of the ZSM-5 zeolite (24.8) is much bigger than the areas of the dealuminated samples, probably due to the transformation of the silanol groups into amorphous forms.

Many conclusions can be drawn from the characteristics of the ZSM-5 and dealuminated ZSM-5 from the (OH) region spectra.

(1) The amount of framework aluminum decreased due to the extraction of aluminum from the zeolitic framework into the acidic solution.

(2) The amount of non-framework aluminum also decreased for the same reason.

(3) The number of silanol groups decreased due to the destruction of silanol group into amorphous forms.

XRD diffractograms provided information about unit cell parameters and crystallinity of the zeolite samples (Table 3). The unit cell parameters and crystallinity of the zeolites were calculated from the XRD diffractograms (Figure 6). The results in Table 3 indicate that the dealumination of ZSM-5 had affected the unit cell parameter and volume unit cells. These values decrease with increasing dealumination time

due to the removal of framework aluminum. These results can be attributed to the slight disorder of lattice structures and the increase in the crystallinity of the dealuminated ZSM-5.

**Table 3. Unit cell parameters and crystallinity of zeolite**

Sample	Unit cell parameter				Crystallinity
	a (Å)	b (Å)	c (Å)	V <sub>uc</sub> (Å <sup>3</sup> )	
ZSM-5	20.07	19.89	12.75	5,088.5	100
DZ-1	19.99	19.88	12.71	5,052.2	118
DZ-2	19.92	19.84	12.68	5,012.0	104
DZ-3	19.91	19.82	12.69	5,007.3	105

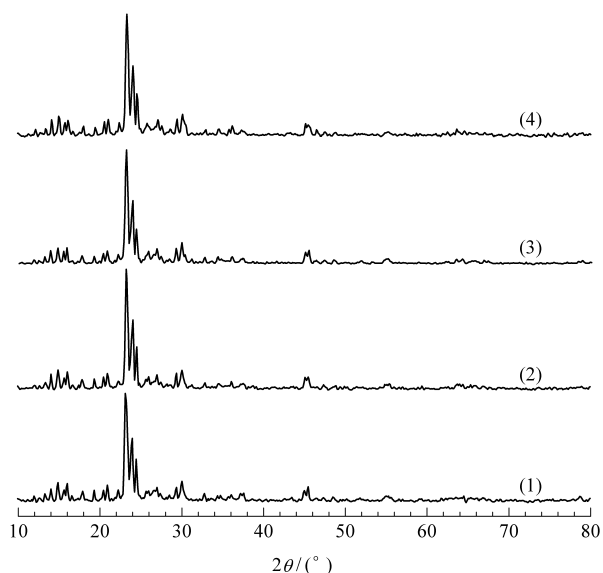


**Figure 6. X-ray diffractogram of (1) ZSM-5, (2) DZ-1, (3) DZ-2, and (4) DZ-3.**

The results from the XRD diffractograms are consistent with the FT-IR analysis. The X-ray diffractograms (Figure 6) indicate that there was no change in the ZSM-5 and dealuminated ZSM-5 crystalline structures. The results in Table 2 and Figure 5, obtained from the FT-IR analysis, suggest that there is a significant change in the number of Si–O–Al forming framework bonds but no destruction of the zeolitic framework as a result of the dealumination treatment.

The crystallinity of the zeolite can be calculated from X-ray diffractograms and is expressed according to [13]. The crystallinities of ZSM-5, DZ-1, DZ-2, and DZ-3 were calculated to be 100, 118, 104, and 105, respectively (Table 3). This result indicates that the crystallinity of the ZSM-5 increases during dealumination because of the reduced amount of framework aluminum. This observation is again consistent with the FT-IR analysis, which illustrates that there is a

significant change in the amount of framework aluminum at the 1,099 cm<sup>-1</sup> frequency band. However, a longer dealumination time leads to a reduction of the crystallinity of the samples. The crystallinities of the samples can be arranged as: DZ-1 > DZ-2 ≈ DZ-3 > ZSM-5.

### 3.2. Catalytic activity of the zeolite

The catalytic activity of ZSM-5 and dealuminated ZSM-5 zeolites were tested for ethylene conversion to liquid hydrocarbons (LHC) via a single step reaction in a packed-bed micro reactor. Fifty ml/min of ethylene with 99.9% purity was reacted at atmospheric pressure and 400 °C. These operating conditions were chosen because the gasoline (C<sub>5</sub>-C<sub>10</sub>) composition was the highest at 94% while the C<sub>11</sub>-C<sub>15</sub> composition was the lowest at 5% when ethylene was reacted over the ZSM-5 zeolite (Figure 7). The experiment was not conducted under 400 °C because it had been reported that the production of oligomers is small at those temperatures [24].

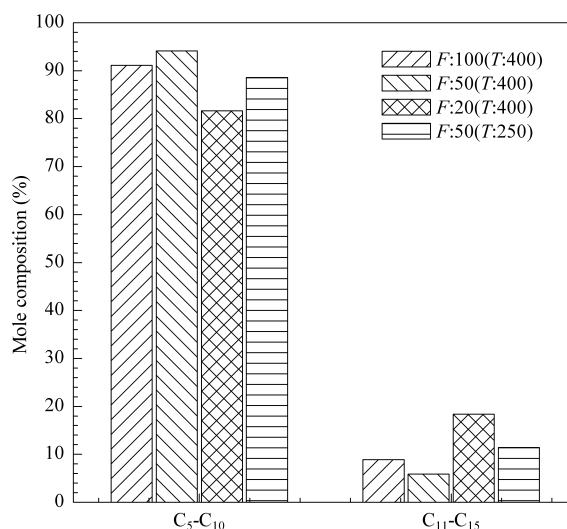


**Figure 7. The composition of liquid fuels under various operation conditions over the ZSM-5 zeolite. T: temperature (°C), F: flow rate (ml/min).**

The ethylene conversion and the compositions of liquid hydrocarbon products are shown in Table 4, and can be summarized according to: C<sub>2</sub>H<sub>4</sub> conversion: DZ-1 > DZ-2 > DZ-3 > ZSM-5, C<sub>3</sub> selectivity: DZ-3 > DZ-2 > DZ-1 > ZSM-5, C<sub>4</sub> selectivity: DZ-3 = DZ-2 > DZ-1 > ZSM-5, C<sub>5</sub>-C<sub>10</sub> selectivity: ZSM-5 > DZ-2 > DZ-1 > DZ-3, C<sub>11</sub>-C<sub>15</sub> selectivity: DZ-3 > DZ-1 > DZ-2 > ZSM-5.

The conversion of ethylene and the selectivities of gas and liquid hydrocarbons are determined by the following equations:

Conversion of ethylene = (Moles of C<sub>2</sub>H<sub>4</sub> reacted / moles of C<sub>2</sub>H<sub>4</sub> in feed) × 100%

Selectivity of hydrocarbons = (Moles of hydrocarbons / moles of C<sub>2</sub>H<sub>4</sub> reacted) × 100%.

**Table 4. Ethylene conversion and selectivity for hydrocarbons of catalysts**

Catalyst	C <sub>2</sub> H <sub>4</sub> conversion (%)	Selectivity of hydrocarbons			
		Gas		Liquid	
		C <sub>3</sub>	C <sub>4</sub>	C <sub>5</sub> -C <sub>10</sub>	C <sub>11</sub> -C <sub>15</sub>
ZSM-5	14.0	0.3	0.0	93.9	5.8
DZ-1	21.7	5.6	0.8	85.9	7.3
DZ-2	18.9	15.9	1.3	76.4	6.3
DZ-3	16.4	17.1	1.3	74.2	7.4

The results of catalyst testing using ZSM-5 and dealuminated ZSM-5 zeolites revealed that the ethylene conversion increased over dealuminated ZSM-5. However, the C<sub>5</sub>-C<sub>10</sub> compositions decreased while the C<sub>3</sub> and C<sub>4</sub> selectivities and C<sub>11</sub>-C<sub>15</sub> compositions increased over the dealuminated ZSM-5.

This result demonstrates that the ethylene conversion is related to the crystallinity of the zeolites and the amount of aluminum in the framework. The latter value had been reduced after the dealumination treatment (Figure 4). Generally, high zeolite crystallinity implies a high surface area [12] and a more active catalyst, which results in a high ethylene conversion. For example, the ethylene conversion of DZ-1 (crystallinity = 118) and ZSM-5 (crystallinity = 100) were 22% and 14%, respectively.

The oligomerization and cracking processes are dependent on the zeolite acidity [7,8]. The self-addition of olefins to form dimmers, trimers, and low polymers is called oligomerization [25]. The amount of framework aluminum is related to the Brönsted acid strength. As the number of the Brönsted acid sites increases, the oligomerization of olefins will also increase.

The results in Figure 8 indicate that the selectivity of C<sub>5</sub>-C<sub>10</sub> hydrocarbons lessened as the number of Brönsted acid sites decreased. The gasoline selectivity of ZSM-5 was about 94% at a N<sub>BAC</sub> value of 2.8 and was reduced to 74% with N<sub>BAC</sub> equal to 0.4 for the DZ-3 sample (Figure 8). Since the number of Brönsted acid sites is the largest for ZSM-5, the oligomerization of ethylene is more efficient over

ZSM-5 zeolite. The results in Figure 8 suggest that successful production of gasoline from ethylene depends partly on the number of Brönsted acid sites and the amount of framework aluminum.

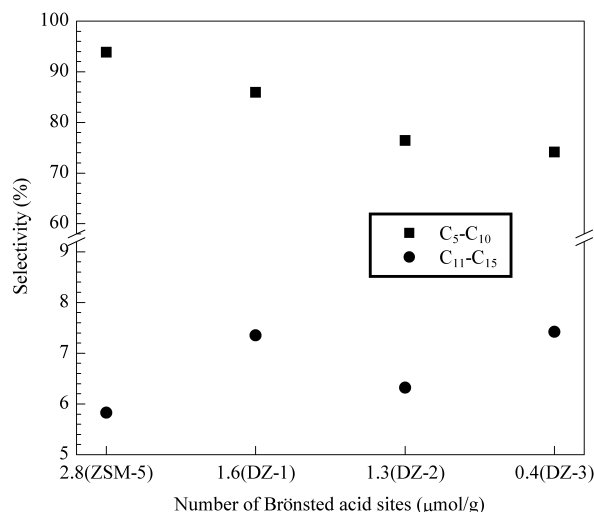
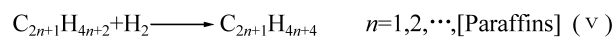
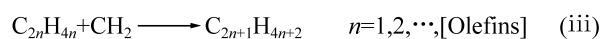
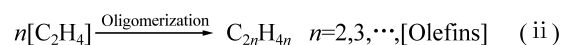
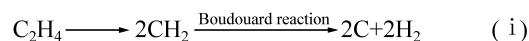


**Figure 8. Effect of the number of Brönsted acid sites on C<sub>5</sub>-C<sub>10</sub> and C<sub>11</sub>-C<sub>15</sub> selectivity over ZSM-5 and dealuminated ZSM-5 under T = 400 °C, F = 50 ml/min.**

The selectivities of C<sub>3</sub> and C<sub>4</sub> gases of dealuminated ZSM-5 (DZ-1 to DZ-3) were higher than ZSM-5 (Table 4). Because the number of Brönsted acid sites in the dealuminated ZSM-5 samples was lower, the oligomerization of ethylene was probably suppressed, resulting in a lower gasoline selectivity and higher gas selectivity compared to ZSM-5.

The reaction path for the oligomerization of ethylene over ZSM-5 and dealuminated ZSM-5 catalysts is proposed in equations (i)-(v).



Ethylene is believed to be dissociated to CH<sub>2</sub>, which then dissociates to C and H<sub>2</sub> by the Boudouard reaction as shown in equation (i). Ethylene also oligomerizes to C<sub>4</sub>H<sub>8</sub>, C<sub>6</sub>H<sub>12</sub>, ... C<sub>2n</sub>H<sub>4n</sub> (equation (ii)). C<sub>2n</sub>H<sub>4n</sub> reacts with CH<sub>2</sub> species to form C<sub>3</sub>H<sub>6</sub>, C<sub>5</sub>H<sub>10</sub>, ... C<sub>2n+1</sub>H<sub>4n+2</sub> (equation (iii)). Finally, the C<sub>2n</sub>H<sub>4n</sub> and C<sub>2n+1</sub>H<sub>4n+2</sub> olefins react with H<sub>2</sub> to form paraffin hydrocarbons (equation (iv-v)).

The product distribution of liquid hydrocarbons

over various zeolites is exhibited in Figure 9. The percentage of paraffin hydrocarbons over ZSM-5 is the lowest (6.98%), but the percentage of olefin hydrocarbons over ZSM-5 is the highest (93.02%). The dealumination of ZSM-5 probably enhanced the dissociation of  $C_2H_4$ , increasing the amount of paraffin hydrocarbons over all the dealuminated ZSM-5 samples. Interestingly, the number of paraffins and olefins did not seem to be affected after 24 hours of dealumination time. The Research Octane Number (RON) was estimated [26] and the results in Table 5 indicate that RON over ZSM-5 is the highest due to its low paraffin content.

**Table 5. Research octane number (RON) of liquid fuel product**

Catalyst	RON
ZSM-5	84
DZ-1	81
DZ-2	83
DZ-3	82

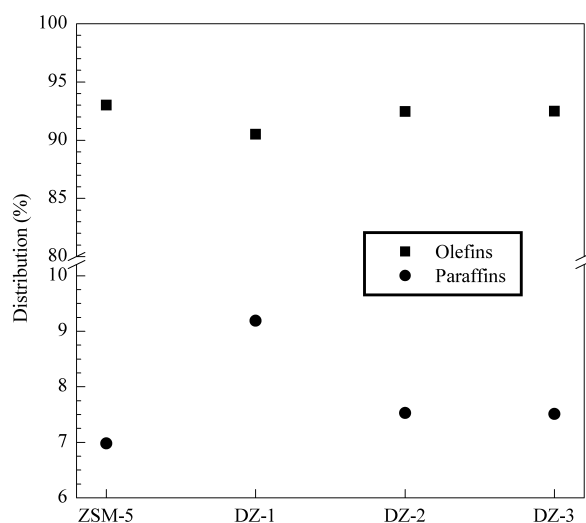


**Figure 9. Product distribution of liquid hydrocarbons over various zeolites.**

#### 4. Conclusion

The dealumination of the ZSM-5 zeolite decreased the framework and non-framework aluminum and the silanol group. However, the purity of the zeolite increased after dealumination. While dealumination of ZSM-5 incremented the ethylene conversion, the gasoline selectivity was reduced. The process to convert ethylene to liquid hydrocarbons is dependent on the

amount of aluminum in the framework, which is related to the Brönsted acid sites and the purity of the ZSM-5. Dealumination time affected the amount of aluminum in the zeolitic framework, the crystallinity of the zeolite, the ethylene conversion, and the gasoline selectivity.

#### Acknowledgements

One of the authors (D.D.A) gratefully acknowledges the financial support received in the form of a research grant (Project No: 02-02-06-0101 and Project No: 09-02-06-0057-SR005/09-07) from the Ministry of Science, Technology and Environment of Malaysia. We would also like to thank Mr. Didik Prasetyoko of the Faculty of Science, UTM for assisting us with the XRD and FT-IR analysis.

#### References

- [1] Han S, Martenak D J, Palermo R E, Pearson J A, Walsh D E. *J Catal*, 1994, **148**: 134
- [2] Weckhuysen B M, Wang D, Rosynek M P, Lunsford J H. *J Catal*, 1998, **175**: 338
- [3] Saidina Amin N A, Ali A. *Jurnal Teknologi*, 2001, **35**(F): 21
- [4] Vasina T V, Preobrazhenskii A V, Isaev S A, Chetina O V, Masloboishchikova O V, Bragin O V. *Kinet Catal*, 1994, **35**: 93
- [5] Saidina Amin N A, Anggoro D D. Proceedings of the Sixth World Congress of Chemical Engineering. Melbourne: Institution of Chemical Engineering in Australia, 2001
- [6] Gnep N S, Doyement J Y, Guisnet M. *J Mol Catal*, 1998, **45**: 281
- [7] Guisnet M, Gnep N S, Vasques H, Ribeiro F R. *Stud Surf Sci Catal*, 1991, **69**: 321
- [8] O'Connor C T, Kojima M. *Catal Today*, 1990, **6**(3): 329
- [9] Woolery G L, Kuehl G H, Timken H C, Chester A W, Vartuli J C. *Zeolites*, 1997, **19**: 288
- [10] Beagley B, Dwyer J, Fitch F R, Mann R, Walker J. *J Phys Chem*, 1984, **88**: 1744
- [11] Kooyman P J, van der Waal P, van Bekkum H. *Zeolites*, 1997, **18**: 50
- [12] Kumar S, Sinha A K, Hegde S G, Sivasanker S. *J Mol Catal A*, 2000, **154**: 115
- [13] Anggoro D D. [Master Thesis]. Malaysia: Universiti Teknologi Malaysia, 1998

- [14] Rhee K H, Brown F R, Finseth D H, Stencel J M. *Zeolites*, 1983, **3**: 344
- [15] Jacobs P A. Carboniogenic Activity of Zeolites. Amsterdam: Elsevier, 1977. 11
- [16] Le Van Mao R, Le T S, Fairbain M, Muntasar A, Xiao S, Denes G. *Appl Catal A*, 1999, **185**: 41
- [17] Loeffler E, Peuker C H, Jerschke H G. *Catal Today*, 1988, **3**: 415
- [18] Jacobs P A, Beyer H K, Valyon J. *Zeolites*, 1981, **1**: 161
- [19] Fierro J L G. *Stud Surf Sci Catal*, 1990, **57**, A186
- [20] Chu C T-W, Chang C D. *J Phys Chem*, 1985, **89**: 1569
- [21] Schuetze F W, Roessner F, Meusinger J, Papp H. *Stud Surf Sci Catal*, 1997, **112**: 127
- [22] Janin A, Maache M, Lavalley J C, Joly J F, Raatz F, Szydowski N. *Zeolites*, 1991, **11**: 391
- [23] Wichterlova B, Tvaruzkova Z, Sobalik Z, Sarv P. *Microporous Mesoporous Mater*, 1998, **24**: 223
- [24] Mariaudeau P, Sapaly G, Naccache C. *Stud Surf Sci Catal*, 1990, **60**: 267
- [25] Parshall G W, Ittel S D. Homogeneous Catalysis. New York: A Wiley-Interscience Publication, 1992. 68
- [26] Protic-Lovasic G, Jambrec N, Deur-Siftar D, Prostenik M V. *Fuel*, 1990, **69**: 525